CAIT-UTC-NC-48

Long-term evaluation of prestress losses in concrete bridges using long-gauge fiber optic sensors

FINAL REPORT
January 2018

Submitted by:

Branko Glisic
Associate Professor

Princeton University
Princeton University E330 EQuad
Princeton, NJ 08544

External Project Manager
Prof. Franklin Moon
Department of Civil and Environmental Engineering
Rutgers University

In cooperation with

Rutgers, The State University of New Jersey
And
New Jersey
Department of Transportation
And
U.S. Department of Transportation
Federal Highway Administration

Disclaimer Statement

The Center for Advanced Infrastructure and Transportation (CAIT) is a National UTC Consortium led by Rutgers, The State University. Members of the consortium are the University of Delaware, Utah State University, Columbia University, New Jersey Institute of Technology, Princeton University, University of Texas at El Paso, Virginia Polytechnic Institute, and University of South Florida. The Center is funded by the U.S. Department of Transportation.

1. Report No.	2. Government Accession No.	3. Recipient's Catalog No.
CAIT-UTC-NC48		

4. Title and Subtitle	5. Report Date
Long-term evaluation of prestress losses in concrete bridges using long-gauge fiber optic sensors	January 2018
	6. Performing Organization Code CAIT/Princeton University
7. Author(s) Branko Glisic	8. Performing Organization Report No. CAIT-UTC-NC-48
9. Performing Organization Name and Address Princeton University Princeton University E330 EQuad, Princeton, NJ 08544	10. Work Unit No.
	11. Contract or Grant No. DTRT13-G-UTC28
12. Sponsoring Agency Name and Address Center for Advanced Infrastructure and Transportation Rutgers, The State University of New Jersey 100 Brett Road Piscataway, NJ 08854	13. Type of Report and Period Covered Final Report 01/07/2016 – 01/31/2018
	14. Sponsoring Agency Code

15. Supplementary Notes
US Department of Transportation, Office of the Assistant Secretary for Research and Technology (OST-R)
1200 New Jersey Avenue, SE
Washington, DC 20590-0001

16. Abstract
Deterioration of infrastructure elements is expected during service life of structures, which necessitates monitoring of its condition. To this end, the overall objective of this research is the creation of a comprehensive suite of methods for the so-called Level III SHM of prestressed concrete structures, where Level III SHM includes detection (Level I), localization (Level II) and quantification (Level III) of unusual structural behaviors, that can serve as the basis for the evaluation of structural health condition (Level IV SHM). The emphasis to long-term prestress losses stems from (1) the steady increase in the use of prestressed concrete in bridge construction in recent years (46% of bridges less than five years old), (2) the fact that they account for 42% of deficient bridges built five years ago or less, and (3) the adverse effect of unexpected prestress losses on the performance and integrity of a prestressed concrete structure. However, long-term monitoring of prestress losses is challenging due to (1) variable on-site conditions, in particular (but not only) temperature, that affect both the structure and the monitoring system, (2) rheological effects in the concrete and prestressing strands, such as creep, shrinkage, and relaxation, that interfere with mechanical effects and affect data analysis, (3) presence of pre-release cracks that affects the distribution of the strain in the structure, and also affects the data analysis, and (4) inherent uncertainties related to the reliability and accuracy of the monitoring system and the estimation of mechanical and geometrical parameters of concrete. The outcomes of the project are (1) the methodology for determination of long-term prestress loss using long-gauge fiber optic sensors, and (2) validation method for long-term temperature and strain measurements used for the analysis.

17. Key Words	18. Distribution Statement
Structural health monitoring, Crack detection, Arrangement of a dense array of sensors, Strain monitoring, Probability of Detection, Large area electronics	

19. Security Classification (of this report)	20. Security Classification (of this page)	21. No. of Pages	22. Price
Unclassified	Unclassified	31	

Form DOT F 1700.7 (8-69)

Acknowledgments

The Streicker Bridge project has been realized with the great help and kind collaboration of several professionals and companies. We would like to thank Steve Hancock and Turner Construction Company; Ryan Woodward and Ted Zoli, HNTB Corporation; Dong Lee and A G Construction Corporation; Steven Mancini and Timothy R Wintermute, Vollers Excavating and Construction, Inc.; SMARTEC SA, Switzerland; Micron Optics, Inc., Atlanta, GA; Geoffrey Gettelfinger; James P Wallace; Miles Hersey; Paul Prucnal; Yanhua Deng; Mable Fok; and Faculty and staff of the Department of Civil and Environmental Engineering. The following students installed the sensors on Streicker Bridge: Chienchuan Chen, Jeremy Chen, Jessica Hsu, George Lederman, Kenneth Liew, Maryanne Wachter, Allison Halpern, David Hubbell, Morgan Neal, Daniel Reynolds, and Daniel Schiffner. Special thanks to Dorotea Sigurdardottir for the permission to use her drawings and to Hiba Abdel-Jaber, Jack Reilly, and Isabel Morris for contributing to this work.

Table of Contents

	Page
DESCRIPTION OF THE PROBLEM	1
APPROACH	2
METHODOLOGY	2
FINDINGS	3
CONCLUSIONS	21
RECOMMENDATIONS	23

List of Figures

Figure 1. Schematic method flowchart. 4

Figure 2. Relationship between ambient temperature (weather tower data from Trenton Airport station, 13 miles southwest of Streicker Bridge) and concrete temperature as measured by a sensor, showing: (a) strong linear relationship between ambient temperature and sensor measurement, and (b) predicted temperature using moving average model and measured temperature: reduced uncertainty as compared to simple linear regression shown in (a). 5

Figure 3. Residuals between the model prediction and the measurements, showing an example of acceptably accurate measurements over the 5-year period; colors denote different datasets. 7

Figure 4. Residuals between the model prediction and the measurements over time for one sensor – an example of malfunction during the five-year period; colors denote different datasets. 8

Figure 5. Residuals between the model prediction and the measurements, showing the progression of the upward trend during the five-year period; colors denote different datasets. 8

Figure 6. Correlation between measurements at the centroid of stiffness of two instrumented cross-sections. 9

Figure 7. Example of sensor network for long-term prestress loss monitoring: two sensors in cross-section (up) and parallel sensors along the structure (down). 12

Figure 8. Schematic representation of prestressed concrete beam. 12

Figure 9. Schematic representation of the proposed method for long-term prestress loss monitoring. 16

Figure 10. Thermally compensated strain at the bottom and top of the cross-section P11, and at its centroid of stiffness. 17

Figure 11. Measurements at the centroid of stiffness of the cross-section at P11 and approximating functions for overall behavior (gray), and rheological strain (black). 17

Page

Figure 12. Estimation of long-term losses at location P11. 18

Figure 13. Monthly plots of three-year prestress loss, 2009 (black) to 2012 (blue). 18

Figure 14. Comparison between prestress force distributions determined from monitoring and four design codes after three years (2009 – 2012); 80% confidence interval for monitoring data is shown in gray color. 19

List of Tables

Table 1. Comparison of general performances of groups of methods applied in monitoring of prestress losses. 11

Table 2. Prestress loss determined from measurements and the code estimates using PCI Simplified Method, AASHTO Approximate Method, AASHTO LRFD Method, and Design*. 20

Table 3. Influence of seasonal effects to prestress loss. 21

DESCRIPTION OF THE PROBLEM

Deterioration of infrastructure elements is expected during service life of structures, which necessitates monitoring of its condition. Currently, structural condition is mostly assessed using visual inspection with most bridges inspected once every two years [1]. The shortcomings of visual inspections are well known and have been widely recognized. To ensure structural integrity, more detailed and frequent monitoring of structural condition is required. While structural health monitoring (SHM) can be used to accomplish this purpose, it is scarcely used on real structures since an efficient approach for its implementation has not been developed yet. Particular challenges represent reliability in damage identification and transformation of SHM data into useful information for the end users. To this end, the overall objective of this research is the creation of a comprehensive suite of methods for the so-called Level III SHM of prestressed concrete structures, where Level III SHM includes detection (Level I), localization (Level II) and quantification (Level III) of unusual structural behaviors, that can serve as the basis for the evaluation of structural health condition (Level IV SHM). The PI proposes the monitoring of long-term prestress losses as an indicative parameter for structural performance and condition of prestressed concrete structures. The particular attention to long-term prestress losses stems from (1) the steady increase in the use of prestressed concrete in bridge construction in recent years (46% of bridges less than five years old [2]), (2) the fact that they account for 42% of deficient bridges built five years ago or less [2], and (3) the adverse effect of unexpected prestress losses on the performance and integrity of a prestressed concrete structure.

One of the most important aspects of a prestressed concrete structure is the distribution of the prestressing force along the structure, both at transfer and in the long term. Time-dependent prestress losses are expected to occur in prestressed concrete due to both strand relaxation and dimensional changes in the concrete caused by creep and shrinkage. Thus, these losses are accounted for in the design based on guidelines set by design codes. However, prestress losses larger than predicted by design can have adverse effects on the structure, where stresses exceed the capacity of the structure at a lower load than predicted. Thus, monitoring of prestress losses will indicate valuable information regarding the performance and health condition of the structure.

However, long-term monitoring of prestress losses is challenging due to (1) variable on-site conditions, in particular (but not only) temperature, that affect both the structure and the monitoring system, (2) rheological effects in the concrete and prestressing strands, such as creep, shrinkage, and relaxation, that interfere with mechanical effects and affect data analysis, (3) presence of pre-release cracks that affects the distribution of the strain in the structure, and also affects the data analysis, and (4) inherent uncertainties related to the reliability and accuracy of the monitoring system and the estimation of mechanical and geometrical parameters of concrete.

The outcomes of the project will be (1) the methodology for determination of long-term prestress loss using long-gauge fiber optic sensors, and (2) validation method for long-term temperature and strain measurements used for the analysis.

APPROACH

The determination of the prestressing force can be accomplished using a wide range of techonologies including vibration methods, ultrasonic methods, acoustoelastic methods, electromagnetic methods, and strain-based methods. We propose a strain-based method due to the direct and well-understood relationship between strain and the prestressing force value; calibration is independent of the structure-type and only dependent on material and geometric properties that can be measured and assessed. We propose instrumentation of the structure with a network of parallel long-gauge fiber optic sensors that measure temperature and strain. Long-gauge strain sensors are used since their long gauge (1) ensures independence of measurement from the influences caused by concrete inhomogeneity, and (2) enables instrumentation of a larger volume of the structure. Fiber optic technology is identified as the most appropriate as (1) it enables long-gauge sensors and (2) it has promise for long-term performance (stability, reliability, and durability).

The method for monitoring of long-term prestress losses thus relies on strain and temperature measurements collected over a period of time. One of the main challenges to the long-term strain monitoring is thermal effects in the structure. To address this challenge, we plan on using data from the structure at the times of the day when the temperature is constant (e.g. midnight to 4 am), such that effects of cross-sectional or longitudinal temperature gradients are minimized. Thus, strain values at that times are principally based on deformations that affect prestress loss.

METHODOLOGY

An overview of the proposed tasks for this project and the time line are listed below, followed by a detailed description of each task. At the end of this section, the references for this proposal are listed.

(1) Methodology for the systematic validation of long-term temperature and strain readings from sensors through comparison to other acquirable and available data (typically weather stations).

- Subtask 1.1: Validation of temperature measurements using a moving average model with ambient temperature as the input parameter (07/01/2016 – 08/31/2016)
- Subtask 1.2: Validation of strain measurements by exploiting the correlations between measurements across different sensors within the same network (09/01/2016 – 11/30/2016)

(2) Systematic methodology that utilizes long-gauge fiber optic strain sensors for the estimation of time-dependent prestress losses along a prestressed concrete structure

- Subtask 2.1: Detailed literature review (12/01/2016 – 01/30/2017)
- Subtask 2.2: Creating methodology based on mechanical models from theory of concrete structures, material science, and design codes (12/01/2016 – 06/30/2017)

(3) Validating the methodologies through application to data from a real-life structure: Streicker Bridge on the Princeton University campus

- Subtask 3.1: Applying methodologies from Tasks 1 and 2 above to data from Streicker Bridge (05/01/2017 – 11/30/2017)

Subtask 3.2: Exploring design codes for numerical simulation of prestress losses for Streicker Bridge and comparison to values from Task 3.1 (05/01/2017 – 11/30/2017)

Deliverables:

- Methodology for validation of long-term temperature as per Task 1 (10/31/2016)
- Methodology for estimation of time-dependent prestress losses along a prestressed concrete structure as per Task 2 (06/30/2017)
- Validation as per Task 3 (11/30/2017)

The first task will serve two purposes: (1) to provide the research community the basis for measurement validation since no long-term validation methods currently exist, to the best of the PI's knowledge, and (2) to ensure that the measurements used in this research are reliable and stable. The second task will develop the theoretical basis for the determination of prestress losses using strain measurements along a structure. The created method will account for uncertainties in mechanical and geometrical properties, and for the possibility of pre-release cracks, defined as cracks that occur before the transfer of prestressing forces [3]. The task will also encompass a survey of the available literature to compare currently available prestress loss monitoring methods. The third task will demonstrate application to a real structure, Streicker Bridge, to show the robustness of the method to environmental influences. Data has been collected on Streicker Bridge since 2009 and long-term data can thus be used to assess time-dependent prestress losses.

FINDINGS

Task 1. Methodology for the systematic validation of long-term temperature and strain readings from sensors through comparison to other acquirable and available data

This first task served two purposes: (1) to provide the research community with the basis for measurement validation since no long-term validation methods currently exist, to the best of the PI's knowledge, and (2) to ensure that the measurements used in this research (for Tasks 2 and 3) are reliable and stable. The two subtasks were to ensure the accuracy and reliability of (1) temperature measurements, and (2) strain measurements. Temperature measurements were validated through comparison to data acquired from the National Oceanic and Atmospheric Administration (NOAA) for ambient temperature. Strain measurements were validated through examining correlations of the sensor measurements across the sensor network. Validation was performed using strain and temperature data from Streicker Bridge at Princeton University campus. To simplify presentation, the method is presented directly through the application on Streicker Bridge, hence a relevant part of Subtask 3.1 is included in this section.

Subtask 1.1. Validation of temperature measurements using a moving average model with ambient temperature as the input parameter

The significant result of this subtask is a method for the validation of temperature measurements from any type of sensors. The method relies on the dependence of temperature inside a concrete structure (or any other type of structure) on ambient temperature. As shown in Figure 1, the method consists of two main tasks: (1) model selection, and (2) malfunction detection. The following subsections detail the two tasks of the method.

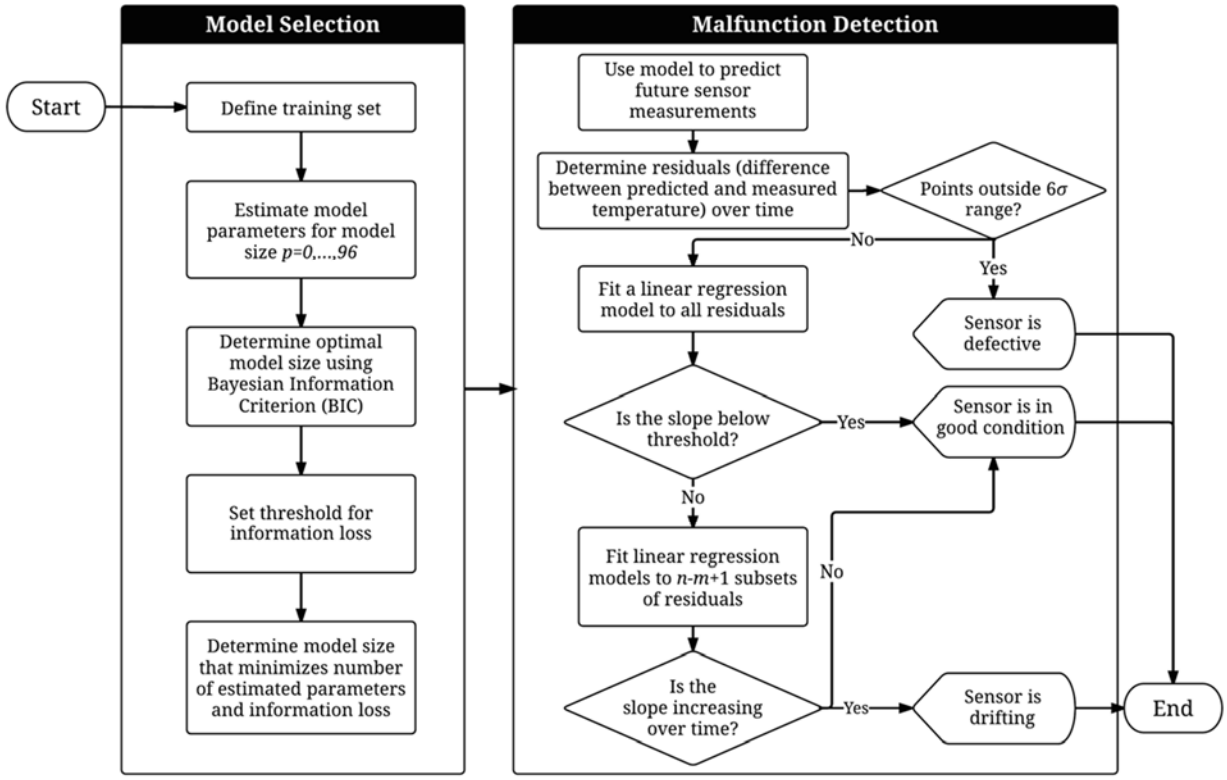

Figure 1. Schematic method flowchart.

Model Selection. Model selection consists of identifying an appropriate class of models and determining all associated parameters. First, a simple linear regression model was selected, where the dependence of temperature inside the structure on ambient temperature is assumed to be linear. As shown in example in Figure 2(a), there is a strong linear correlation between ambient temperature and sensor measurement. However, there is large uncertainty in predicting sensor measurements using ambient temperature since at any given ambient temperature, there is a wide range in which the sensor measurement can fall (for example in Figure 2(a), this range is approximately 15°C). This uncertainty is due to the assumptions of the model; a linear regression model assumes no delay between the change in ambient temperature and the response of the temperature inside the structure. The thermal inertia of the structure's material, however, contradicts this assumption. Thus, the delay between the ambient temperature change and the structure's temperature change causes large uncertainty. To improve results, a moving average model is proposed, where the structure's internal temperature is defined as a weighted average of the ambient temperature over the past p hours, as given in equation (1).

$$T_{\mathrm{in},k} = \sum_{j=0}^{p} b_j T_{\mathrm{amb},k-j} \tag{1}$$

where $T_{\mathrm{in},k}$ and $T_{\mathrm{amb},k}$ are the internal structure's and ambient temperature values at time point k, respectively, p is the length of the memory of the model, and b_j ($j=0,1,2\ldots p$) are the least squares coefficients of the linear regression.

As shown in Figure 2(b), a moving average model significantly reduces uncertainty, allowing for a more accurate prediction of future sensor measurements.

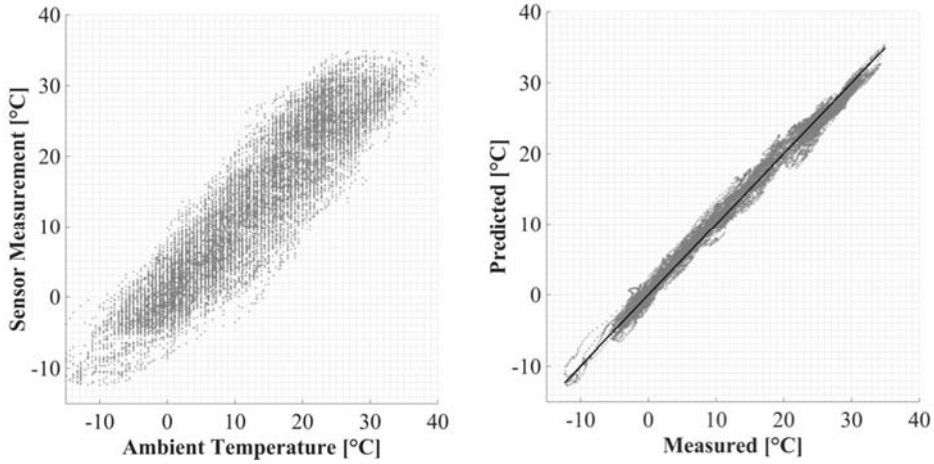

(a) (b)

Figure 2. Relationship between ambient temperature (weather tower data from Trenton Airport station, 13 miles southwest of Streicker Bridge) and concrete temperature as measured by a sensor, showing: (a) strong linear relationship between ambient temperature and sensor measurement, and (b) predicted temperature using moving average model and measured temperature: reduced uncertainty as compared to simple linear regression shown in (a).

To determine the parameters of the model, namely the size of the model p and coefficients of regression b_j, a training period must first be defined. It is recommended to use a training period long enough such that the measurements cover the full range of expected measurements, while balancing the trade-off of assuming the sensor measurements are accurate for an extended period of time. By definition, the sensor is assumed to function properly throughout the training period and the model parameters are determined based on this period. It is recommended to use at least one year of measurements such that the full temperature range of the structure is experienced by the sensor. Additionally, for sensors with stable long-term performance such as fiber optic sensors, it is reasonable to assume that they produce accurate measurements for at least one year after installation. Thus, in this study, a training period of one year is adopted.

To determine an appropriate model size, models with varying sizes are generated and compared. This study recommends generating models with sizes ranging from zero (using only the current ambient temperature to predict sensor measurements) to 96 hours (using the past 96 hours of measurements in addition to the current ambient temperature to predict sensor measurements). Once a sufficient number of models have been generated, the models can be compared. The comparison is based on information theory to evaluate the loss of information (increase in uncertainty) incurred by using a smaller model size. The purpose is to reduce the model size and thus complexity while maintaining a reasonably accurate model. Two criteria commonly used to evaluate model complexity are the Akaike Information Criterion (AIC) [4], and the Bayesian Information Criterion (BIC) [5]. While AIC is more theoretically founded than BIC, the latter produces reasonably accurate results while penalizing model complexity more heavily, which is desired in this application [6]. Once an optimal model size is selected by minimizing the BIC, the model size can be further reduced using engineering judgment. By setting a threshold on the increase in standard deviation as a percentage of the standard deviation for the optimal model size as determined by BIC. The model with the smallest size that meets the threshold criterion is then selected. In this study, a threshold of 10% is used and model sizes are

evaluated in 12-hour increments. Model sizes for temperature measurements in Streicker Bridge where between 30 and 36 hours.

Malfunction Detection. Once the model is created, future sensor measurements can be predicted using the corresponding ambient temperature values. The goal is to validate measurements by examining the discrepancies between the predicted and measured temperature at the sensor location. This is done by analyzing the residuals' values in time to identify their pattern over time, if any. Two types of malfunction are identified and characterized in this study: (1) defect resulting in erroneous measurements, and (2) minor drift resulting in slightly inaccurate measurements.

First, to identify defect, a threshold must be set on residuals, such that if it is exceeded, the sensor is classified as defective and measurements are deemed inaccurate. For this purpose, a threshold of six standard deviations is used (standard deviation of residuals in the training period). The six-standard-deviation threshold was chosen based on the fact that distributions of residuals for the training sets were typically Gaussian, and thus, for properly functioning sensors, the residuals are expected to be within the threshold with very high confidence (99.999998%, i.e., practically 100%). A very high level of confidence is needed in order to avoid false identifications of sensor malfunctioning, especially in the cases of incomplete data sets that are frequently present in real-life settings, and occasionally large differences between temperature in the air and concrete generated by extreme weather condition. Data from defective sensors is deemed unusable and thus must be ignored or replaced. To replace data, the model created can be used, in addition to possibly using linear combinations of measurements from other sensors on structure, if any. However, this is beyond the scope of this study and will not be explored in more depth.

If all measurements are within the six standard deviation range, the next step is to determine whether or not the sensor is exhibiting minor drift, i.e., evaluate the stability of measurements. Stability is assessed by fitting a linear regression model to all residuals over time and examining the significance of the slope of the line. A slope that exceeds the threshold indicates that measurements are not stable and exhibit drift over time. The threshold is determined based on the purpose of monitoring and the uncertainty that can be tolerated as a result. For example, if the purpose of temperature monitoring is to evaluate mechanical strain in a structure, an uncertainty of 0.5°C per year can be tolerated since that results in an uncertainty in strain measurement of 6με/year based on a thermal expansion coefficient of 12με/°C for structure's material. This strain uncertainty is minute compared to the order of magnitude of strain changes in concrete. Thus, a slope below the threshold of 0.5°C/year indicates the sensor's stability is acceptable.

A slope that exceeds the threshold, however, requires more analysis to quantify drift and determine when it starts to occur. This closer examination is achieved by performing linear regression over overlapping subsets of the data, such that slopes from multiple linear regressions are evaluated to examine progression of drift over time. It must be noted that the residuals are expected to fluctuate over time because the model will systematically under-predict or over-predict temperature based on the season. Thus, if temperature measurements are not continuously recorded (i.e., the datasets feature gaps), residuals from datasets from some years might be skewed more towards a certain temperature range than another, thereby introducing bias in the residuals as well and the resulting linear regression slope. Therefore, the length of the subsets over which linear regression for residuals is performed (m years) depends on the length of the available dataset (n years) and the distribution of the collected data every year. A longer subset (larger m) provides less bias, but it must be noted that as m approaches n, the number of linear regressions performed decreases, providing less slopes for comparison

and assessment. Thus, the requirements of decreasing bias and producing a sufficient number of linear regression slopes for assessment must be balanced such that the latter is at least three, while not compromising the former. Then, the slopes are evaluated and compared over time; if the slope continuously deviates in the same direction, the sensor is classified as exhibiting drift from the subset at which the slope exceeds the slope threshold previously set. Measurements can then be corrected by eliminating the trend described by the linear regression for the subsets at which drift is deemed to exist.

Part of Subtask 3.1. Detection of sensor malfunction in Streicker Bridge monitoring system

Both types of malfunction discussed above were detected in temperature sensors from Streicker Bridge: (1) defect, and (2) measurement drift. First, to illustrate the procedure for malfunction detection, residuals (difference between model prediction and sensor measurements) for a sensor with accurate measurements over a period of five years (2009-2014) are presented in Figure 3. As previously mentioned, thresholds for defect are set at 6 standard deviations from the mean, as defined by the training set standard deviation. For the sensor measurements shown in Figure 3, there are no points outside the bounds and thus, the sensor is not defective. Additionally, residuals do not increase significantly over time, as given by the slope of 0.35°C per year (less than the 0.5°C per year threshold). Therefore, the sensor measurements are considered to be acceptably accurate. Most of the sensors installed on the bridge exhibit similar behavior.

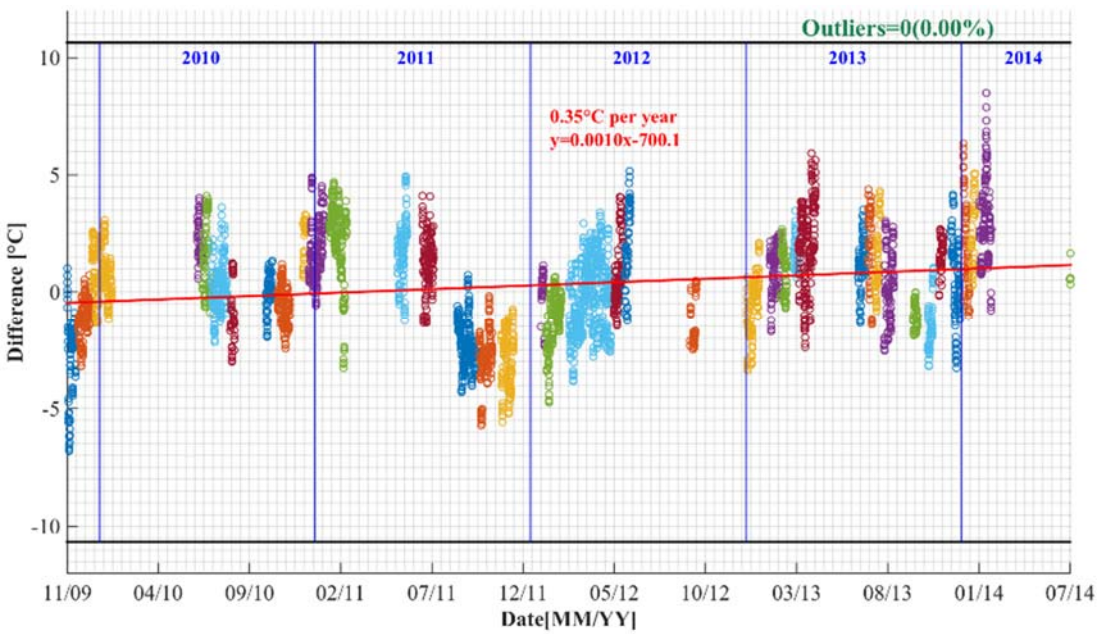

Figure 3. Residuals between the model prediction and the measurements, showing an example of acceptably accurate measurements over the 5-year period; colors denote different datasets.

Defect. Other sensors, however, experience defect during the five-year period, such as the sensor shown in Figure 4, where some measurements in 2013 significantly deviate from the model predictions, thereby resulting in outliers (data that deviates from the model prediction by more than 6 standard deviations) that compose approximately 6% of the data. For this sensor, datasets from this period are inaccurate, and must be excluded from the data analysis. However, other datasets still correspond to the model very well and can be used for future analysis.

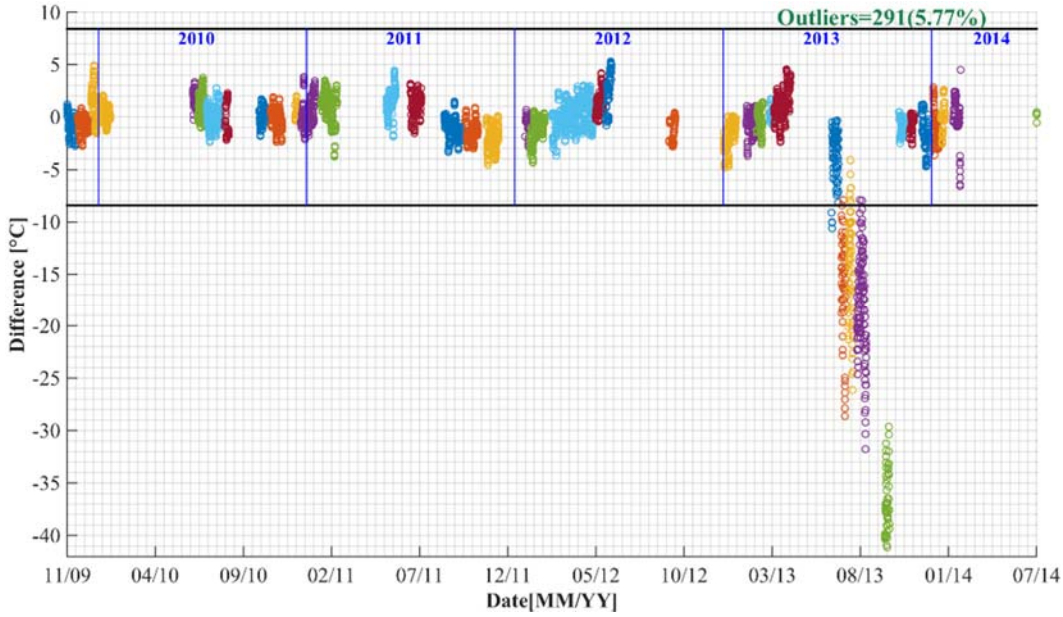

Figure 4. Residuals between the model prediction and the measurements over time for one sensor – an example of malfunction during the five-year period; colors denote different datasets.

Minor Drift. Some sensors do not experience defect, but their measurements tend to drift away from the model slowly over time, as shown in Figure 5. Based on the three linear regressions, the slope seems to increase over time. Additionally, it can be seen that the slope is not significant for the first three-year period, indicating that drift does not occur until the end of 2012. After 2012, the slope (i.e., the drift) begins to increase, first to 0.81°C through 2013, and then 1.38°C through 2014. Measurement correction can thus be performed by fitting a line to the upward trend seen in years 2013 and 2014 and compensating measurements for the trend.

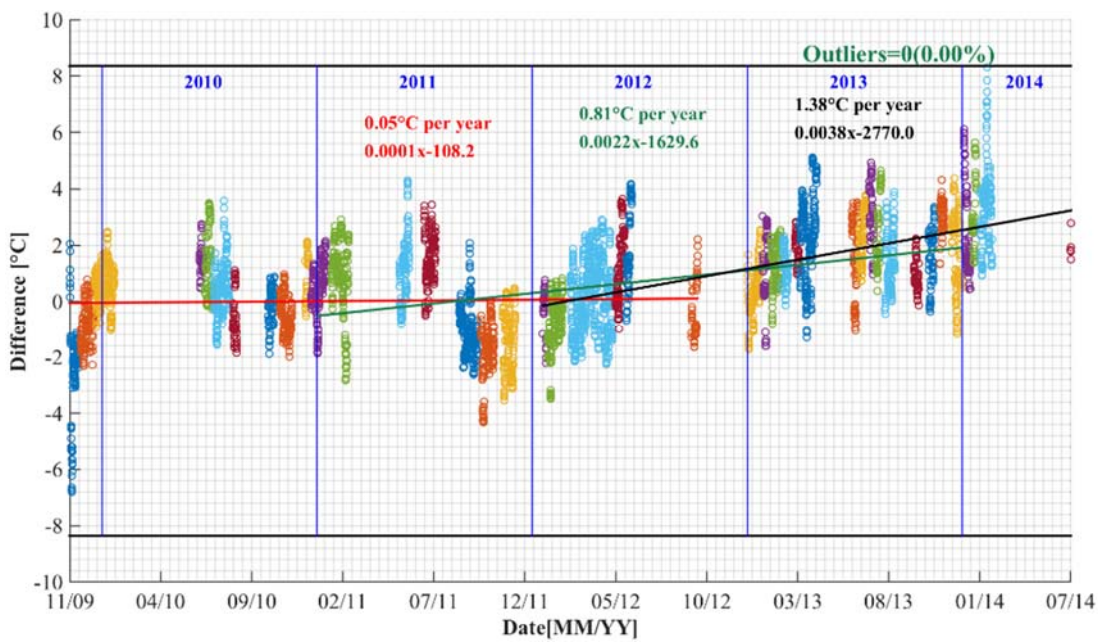

Figure 5. Residuals between the model prediction and the measurements, showing the progression of the upward trend during the five-year period; colors denote different datasets.

Subtask 1.2. Validation of strain measurements in Streicker Bridge

As is the case frequently in SHM applications, direct validation of strain measurements was not possible due to the unavailability of a redundant monitoring system for comparison. Instead, validation was performed based on correlations between sensor measurements. Sensor measurements from different cross-sections along the southeast leg of Streicker Bridge were compared to one another.

To facilitate comparison without including effects of bending due to loads, sensor measurements at each cross-section were interpolated at the centroid of stiffness of each cross-section. An example of a comparison for measurements in the five-year period 2009–2014 is shown in Figure 6. As shown, the measurements at the centroids of stiffness of the two instrumented locations correspond well to each other, with a slope for the relation of 1.01, indicating that measurements from the sensors are sufficiently accurate. Based on similar comparisons for other cross-sections, all slopes for the relations between the sensors are between 0.97 and 1.03.

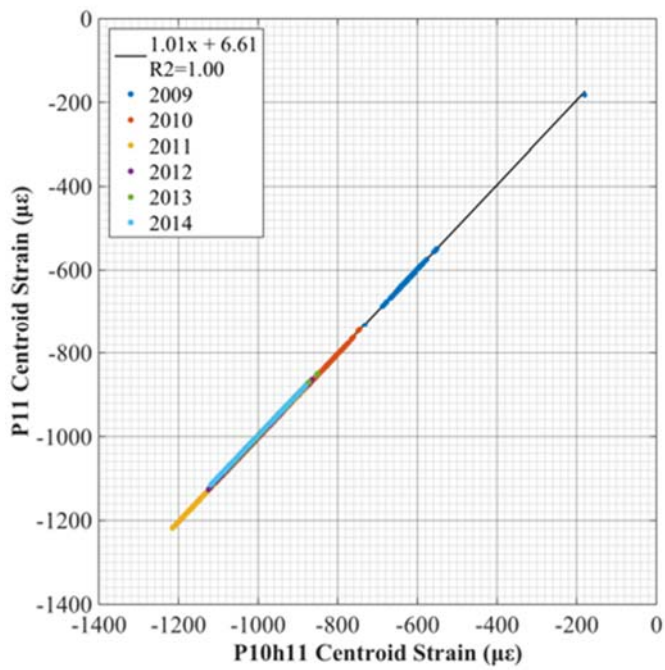

Figure 6. Correlation between measurements at the centroid of stiffness of two instrumented cross-sections.

Task 2. Systematic methodology that utilize long-gauge fiber optic strain sensors for the estimation of time-dependent prestress losses along a prestressed concrete structure

This second task aimed at (1) informing the research and providing the research community with the state-of-the-art (review) on the current methods for determination of long-term prestress losses, and (2) creating new, systematic and rigorous method for long-term prestress loss monitoring. Both of these subtasks were accomplished.

Specific objectives

For the first subtask, the specific objective was identification of various methods currently applied in long-term prestress monitoring, and evaluation of their performance. For the second subtask, the specific objective was to create a method for prestress loss determination based on monitoring results, combined with theory of concrete structures, material science, and design codes.

Subtask 2.1. Detailed literature review

This literature review provides practitioners with various methods for prestress loss monitoring, and their performances. In general five groups of methods were identified: (1) vibration methods, (2) impedance-based methods, (3) elasto-magnetic methods, (4) acoustic methods, and (5) strain-based methods. These methods were evaluated using the following criteria: (A) sensitivity to prestress force changes, (B) effects of environmental factors, (C) feasibility of instrumentation, and (D) applicability to real-life structures. More than 100 papers were consulted, and Table 1 summarizes the findings listed below:

- Vibration methods did not appear appropriate for monitoring prestress losses due to the contradicting arguments regarding their sensitivity to the prestressing force change. In addition, the global nature of vibration monitoring, as well as changes in boundary conditions, environmental conditions, and other types of damage practically limit their applicability.

- Impedance-based methods, while showing a promise for detecting local changes in pre-stressing forces, are limited due to required calibration, large number of sensors needed, and cross-sensitivity with temperature. However, the biggest limitation is current inability to install the sensors directly on the concrete surface.

- Elasto-magnetic methods have great potential to monitor absolute force in tendons even if installed after the construction. Calibration is required, but it can be performed in laboratory. However, the limitation is their size that makes them suitable to be installed mostly on external tendons, while embedment in concrete structures is currently impractical.

- Acoustoelastic methods are currently not suitable for prestress loss monitoring, due to low sensitivity to prestressing force changes. The issue is amplified by the fact that attenuation of stress waves in concrete is high, which limits the application to ungrouted, shorter tendons.

- Strain-based methods were found to have the strongest promise for monitoring prestressing losses due to the maturity of the sensing technologies and the well-established relationship between strain and stress. It is necessary to instrument the structure during construction, which is generally feasible due to availability of embeddable sensors (e.g., vibrating wire based or fiber optics based).

Table 1. Comparison of general performances of groups of methods applied in monitoring of prestress losses

	Vibration	Impedance	Elasto-magnetic	Acoustoelastic	Strain
Sensitivity to prestress force changes	Debatable	High (locally)	High	Low	High
Effects of environmental factors	High	High	High (can be calibrated)	Not explored	High (can be compensated)
Feasibility of instrumentation	High	High	Low	High	High
Applicability to real-life structures	Unfeasible	Feasible with calibration	Feasible with calibration	Feasible with attenuation considerations	Feasible

Subtask 2.2. Creating methodology based on mechanical models from theory of concrete structures, material science, and design codes

This significant result of this subtask is a strain-based method for determination of long-term prestress losses. The method relies on strain and temperature measurements, and for best performance requires the sensors to be embedded in concrete during construction. If installed after construction, the method can identify losses that occur after the moment of installation, but not prior to that moment. The method is designed for beam-like structures working under assumption of linear theory.

The method consists of three main components: (1) design of sensor network, (2) derivation of analytical model for data analysis, and (3) uncertainty analysis. As a part of validation, method was preliminary applied on Streicker Bridge, pedestrian bridge on Princeton University campus.

Design of sensor network. Design of sensor network has two components – identification of type of sensor and identification of locations where the sensors should be placed. Two most suitable type of sensors identified for long-term strain monitoring are vibrating wire sensors (VW) and long-gauge fiber optic sensors (FOS). VW sensors are more affordable, but suffer from short-gauge errors and sensitivity to electromagnetic interference. FOS are more expensive, but long gauge length makes them particularly suitable for monitoring concrete structures, and insensitivity to EMI makes them reliable in the long term. Both types of sensors are suitable for long-term strain monitoring, and the choice depends on project specifications. At each location where the strain sensor is installed, an additional temperature sensor must be installed in order to compensate the sensor for temperature effects and to separate thermal strain in the structure.

The method presented in this report uses strain value determined in the centroid of stiffness of the cross-section (see next subsection). Thus, it is necessary to have at least two sensors parallel to centroid line in each instrumented cross-section, assuming that Bernoulli hypothesis is valid, and that uniaxial bending is dominant. For redundancy and improved accuracy purposes, but also in the case of bi-axial bending, it is recommended to have more than two sensors in the cross-section, budget permitting.

Finally, pairs of parallel sensors should be distributed along the structure, so that they cover all cross-sections of local maximum and minimum (maximum negative) bending moments,

extremities of the beam (where the prestressing force is applied), abrupt changes in the cross-section (if any), and at least one inflection point (i.e., where damage is less likely to occur, and this point can be used for reference purposes). An example of sensor network with the above characteristics is shown in Figure 7.

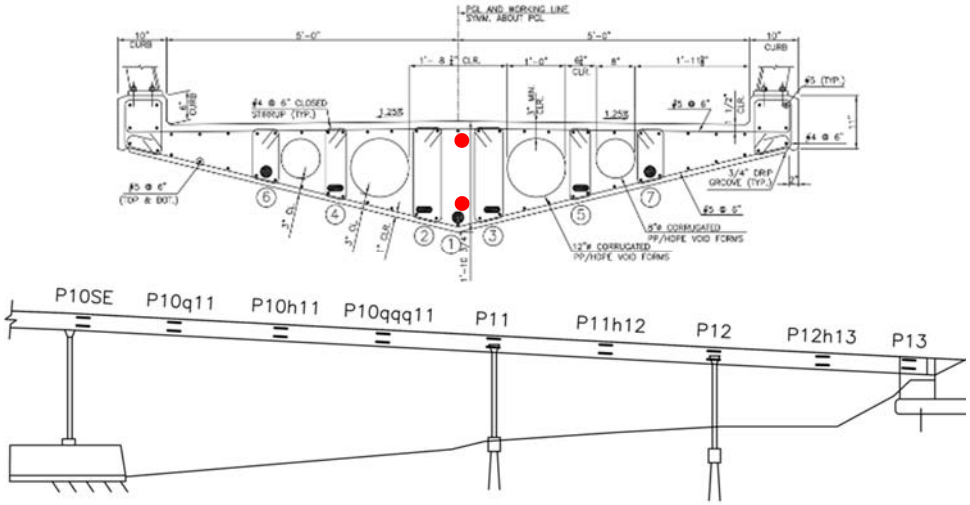

Figure 7. Example of sensor network for long-term prestress loss monitoring: two sensors in cross-section (up) and parallel sensors along the structure (down).

Analytical model

Equations (1) and (2) show the compatibility and equilibrium conditions for a prestressed concrete beam (see Figure 8).

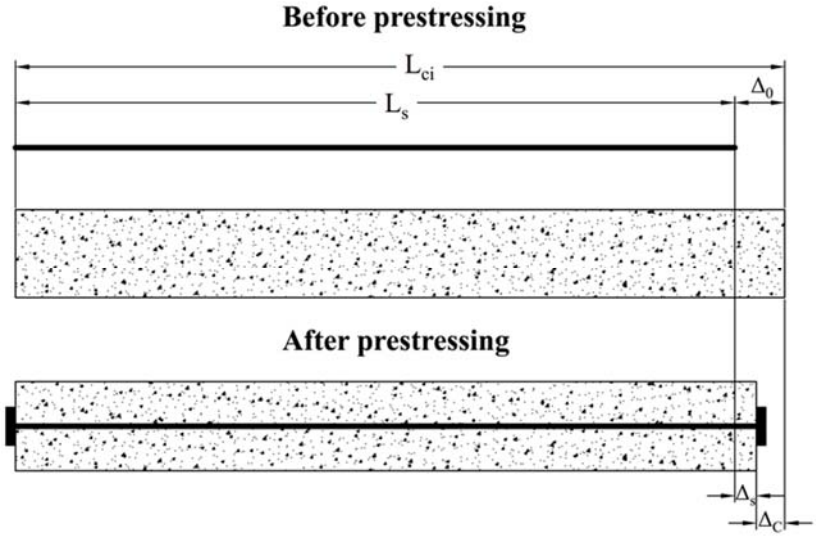

Figure 8. Schematic representation of prestressed concrete beam.

Strain measurements in concrete reflect dimensional changes due to creep and shrinkage (rheological strain in concrete), and due to relaxation of prestressing strands.

$$\Delta_S - \Delta_C = \Delta_0 \qquad (2)$$

$$F_C = -F_S \tag{3}$$

where F_S and F_C are the forces due to prestressing in the steel strands (tensile) and the concrete cross-section (compressive), respectively, and Δ_S and Δ_C denote the change in length of the steel strand (elongation) and concrete beam (shortening), respectively (all parameters are presented in Figure 8).

Equations (2) and (3) are translated in (4) and (5), respectively, so the forces and changes in lengths are replaced with strain.

$$\varepsilon_S L_S - \varepsilon_C L_{Ci} = \Delta_0 \tag{4}$$

$$\varepsilon_C E_C A_C = -\varepsilon_S E_{PS} A_{PS} \tag{5}$$

where ε_S and ε_C are the strains at the prestressing strands and centroids of stiffness of the concrete cross-sections, respectively, and $E_{PS}A_{PS}$ and $E_C A_C$ are the axial stiffnesses of the prestressing strands and concrete, respectively.

The changes in the length caused by rheological strain are given in (6).

$$\varepsilon_S L_S - \varepsilon_C L_C = \Delta \tag{6}$$

By manipulating Equations (4-6), one obtains:

$$\varepsilon_C = -1 + \frac{(n+1)}{\Delta + L_S(n+1)} L_S \tag{7}$$

where $n = \frac{E_C A_C}{E_{PS} A_{PS}}$.

Taking into account to the change in the modulus of elasticity of the concrete during the early-age, (7) is can be transformed into (8).

$$\Delta\varepsilon_C = -1 + \frac{(n(t)+1)}{\Delta'(t) + L_S(n(t)+1)} L_S \tag{8}$$

where $\Delta\varepsilon_C$ is the change in strain between two successive measurements, which are assumed to be performed during a period which is short enough, so the modulus of elasticity is assumed to be constant, $n(t) = \frac{E_C(t)A_C}{E_{PS}A_{PS}}$, and $\Delta'(t)$ is the change of Δ between two measurements.

$\Delta'(t)$ is determined using strain measurements from the sensors as presented in (9). All other parameters in Equation (8) represent geometrical and mechanical properties of materials.

$$\begin{aligned} \Delta'(t) &= \Delta(t) - \Delta(t - \Delta t) \\ \Delta(t) &= \Delta_0 + L_{Ci}\varepsilon_R - L_S \tilde{\varepsilon}_{Relax} \end{aligned} \tag{9}$$

where ε_R is the rheological strain at the centroid of stiffness of the concrete cross-section, while $\tilde{\varepsilon}_{\text{Relax}} = \frac{\sigma_{\text{Relax}}}{E_{\text{PS}}}$ is a fictitious – "equivalent" – strain term that reflects the change in strain in the centroid of stiffness of the concrete due to strand relaxation (σ_{Relax}).

Given that the lengths L_{Ci} and L_S are approximately equal, L_S can be approximated by L_{Ci} and Equation (9) becomes (10).

$$\Delta(t) = \Delta_0 + L_{\text{Ci}}\left(\varepsilon_{\text{R}} - \tilde{\varepsilon}_{\text{Relax}}\right) \tag{10}$$

The initial values of L_S and Δ_0 can be determined by setting time of prestressing $t=t_0$ in (8). Finally, the prestressing force F_C in the concrete cross-section is given by (11).

$$F_{\text{C}} = \sum_{i=1}^{m} \Delta\varepsilon_{\text{C},i} E_{\text{C}}(t_i) A_{\text{C}} \tag{11}$$

where $t_{1,2,\ldots,m}$ are the time steps of measurements (short enough such that the modulus of elasticity of the concrete is assumed to be constant between them).

The strain at the centroid of stiffness, used in (11), is determined from measurements of parallel sensors by combining Equations (12) (to find curvature in cross-section) and (13).

$$\kappa = \frac{\varepsilon_{\text{b}} - \varepsilon_{\text{t}}}{h} \tag{12}$$

$$\varepsilon_{\text{CS}} = \varepsilon_{\text{t}} - \kappa y_{\text{t,CS}} \tag{13}$$

where κ is the curvature of the cross-section, ε_b and ε_t are the measured strains at the bottom and top sensor locations, respectively, h is the vertical distance between the two sensors, ε_{CS} is the strain at the centroid of stiffness, and $y_{t,CS}$ is the distance between the top sensor and the centroid of stiffness.

Given that the strain is considered only at the centroid of stiffness, bending effects due to loads and prestressing are filtered out, and only longitudinal strain, directly related to prestress force, remains. Assuming uniaxial bending and no damage to the structure, longitudinal strain could contain components due to thermal strain and the loss of prestressing $\left(\varepsilon_{\text{R}} - \tilde{\varepsilon}_{\text{Relax}}\right)$. Thus, it is necessary to filter out thermal effects. However, due to effects of non-linear thermal gradients across the cross-section, simply removing thermal strain by applying Equation (13) would not be sufficiently accurate. Thus, it was decided to minimize influence of nonlinear temperature effects by considering only strain measurements from measurements performed at times at which the cross-section was considered to be under approximately constant temperature, which was in this project limited to 1°C. For these measurements, the Equation (14) is applied to remove temperature effects.

$$\varepsilon_{\text{compensated}} = \varepsilon_{\text{measured}} - \alpha_{\text{T}}\left(T_{\text{measured}} - T_{\text{ref}}\right) \tag{14}$$

where $\varepsilon_{compensated}$ is there thermally-compensated strain, $\varepsilon_{measured}$ is the measured strain, $T_{measured}$ is the measured temperature (at the time of the measured strain), and T_{ref} is the reference temperature.

To compare measurements at different sensor locations and to deal with the common issue of missing measurements, an interpolation function is fit to each sensor measurements. Since the seasonal effects may remain at the centroid of stiffness due to changes affecting other structural elements (e.g., thermal changes in bridge columns, the changes in foundation conditions, etc.), a two-part function is used to account for both rheological strain and seasonal effects. This function is given in Equation (15). The exponential part is used to approximate the effects of creep, shrinkage and strand relaxation, while the sine function is used to model the effects of seasonal changes to the structure. Consequently, only the first function is used to determine long-term prestress losses. The second function, could be used to assess the integrity of the structure as it can cause variations in the prestressing force seasonally.

$$\varepsilon = \left(A_1 e^{A_2 t} + A_3 e^{A_4 t}\right) + \left(B_1 \sin\left(\frac{2\pi}{365} t + B_2\right) + B_3\right) \tag{15}$$

where $A_{1,2,3,4}$ and $B_{1,2,3}$ are the parameters of the exponential and sine function, respectively, and t is the time after prestressing, in days.

Finally, given that strain measurements tend to stabilize over time as rheologic effects stabilize, the exponential function given in (14) has to be truncated and replaced with constant value at appropriate time. For practical purposes, the exponential function is assumed to stabilize at a time at which its value reaches the average of the last year of measurements, and after that time it is represented by a constant.

Uncertainty analysis

To make possible direct comparison between measured prestress losses and those predicted from design codes, rigorous uncertainty analysis has to be performed. The two sources of uncertainties are uncertainties in measurements and uncertainties in parameter estimations. The former are related to the monitoring system and their estimation is supplied by SHM system manufacturers. The latter include uncertainties in the locations of the centroids of stiffness, cross-sectional areas, lengths of concrete and prestressing steel members, and moduli of elasticity. Uncertainties are propagated by applying uncertainty propagation formula given in Equation (16) to Equation (11), which results to Equation (17).

$$[\delta(y)]^2 = \left[\frac{\partial y}{\partial x_1}\delta(x_1)\right]^2 + \left[\frac{\partial y}{\partial x_2}\delta(x_2)\right]^2 + \ldots + \left[\frac{\partial y}{\partial x_n}\delta(x_n)\right]^2 \tag{16}$$

where y is a function of x_1, x_2, …, x_n and $\delta(x)$ is the uncertainty in variable x.

$$(\delta F_C)^2 = \left[\bar{E}_C A_C \delta\left(\sum_{i=1}^{m} \Delta\varepsilon_{C,i}\right)\right]^2 + \left[A_C \delta\left(\bar{E}_C\right)\sum_{i=1}^{m} \Delta\varepsilon_{C,i}\right]^2 + \left[\bar{E}_C \delta\left(A_C\right)\sum_{i=1}^{m} \Delta\varepsilon_{C,i}\right]^2 \tag{17}$$

where $\bar{E}_C$ is the equivalent average modulus of elasticity of the concrete given by $\bar{E}_C = \dfrac{F_C}{A_C \sum_{i=1}^{m} \Delta\varepsilon_{C,i}}$.

The method described in this sections is summarized in Figure 9.

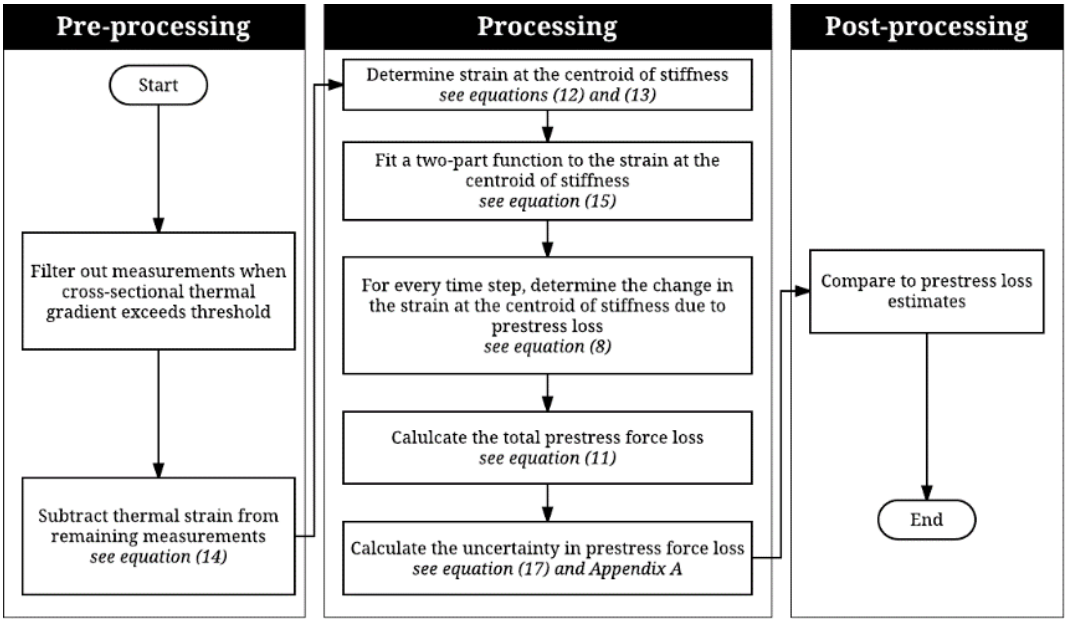

Figure 9. Schematic representation of the proposed method for long-term prestress loss monitoring.

Task 3. Validating the methodologies through application to data from a real-life structure: Streicker Bridge on the Princeton University campus

Subtask 3.1. Applying methodologies from Tasks 1 and 2 above to data from Streicker Bridge

Application of methodology relative to Task 1 was presented in the first section above, where Task 1 was presented in detail.

Methodology relative to Task 2 is being applied to Streicker Bridge at Princeton University campus. The bridge was instrumented with FOS embedded in concrete during construction. Sensor network on the bridge is presented in Figure 7. Figure 10 shows thermally-compensated strain measurement at location P11 (after they were filtered for constant thermal gradients and longitudinal thermal strain). Strain at centroid of stiffness was calculated using Equation (13) and shown in the same figure.

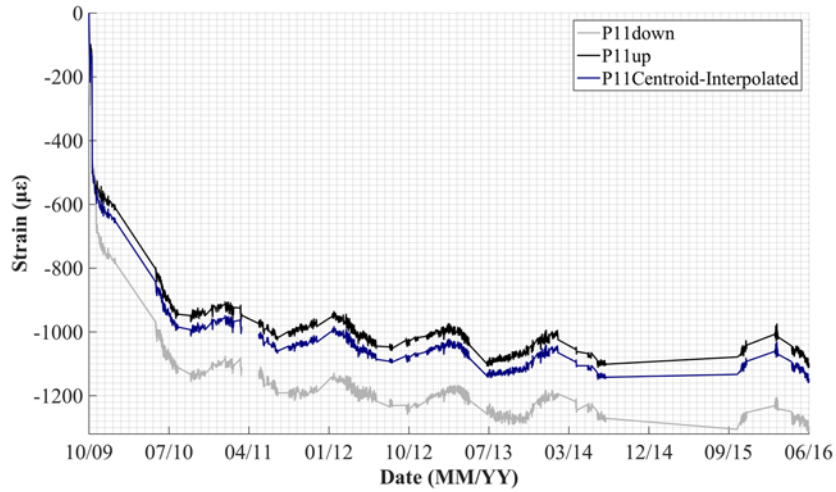

Figure 10. Thermally compensated strain at the bottom and top of the cross-section P11, and at its centroid of stiffness.

A function of the form presented in Equation (15) is fit to the interpolated measurements for the centroid of stiffness, as shown in Figure 11. It was assumed that rheologic effects stabilize at the time when its value reaches the average of the last year of measurements (August 2015 for P11), and measurements are assumed to be constant after that time.

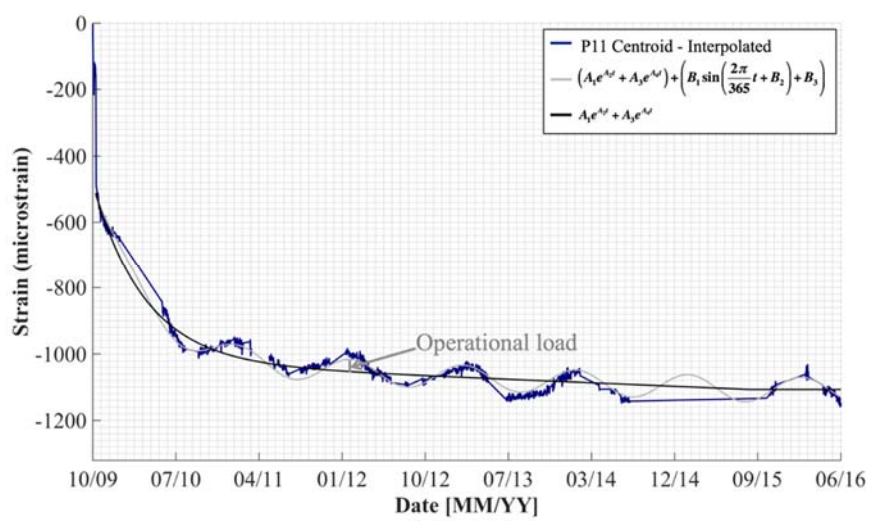

Figure 11. Measurements at the centroid of stiffness of the cross-section at P11 and approximating functions for overall behavior (gray), and rheological strain (black).

Using the function from Figure 11 and Equations (8), (10), and (11), it is possible to determine the absolute magnitude of the force from the time of post-tensioning. Figure 12 shows the 7-year results for location P11. As shown in the figure, approximately 70% of total loss occurs at post-tensioning due to friction, anchorage loss, and elastic shortening. Long-term losses represent approximately 8% of total prestressing force, a significant proportion of which (more than 50%) occurs in the first six months.

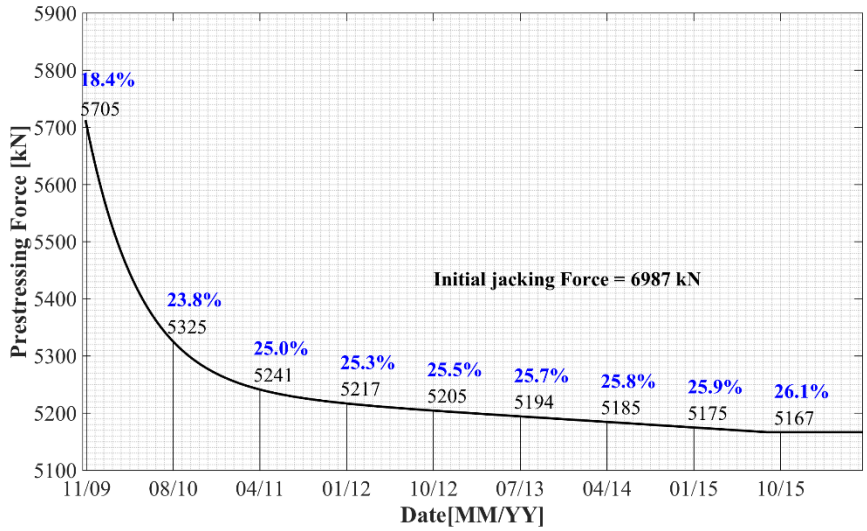

Figure 12. Estimation of long-term losses at location P11.

The application of the method to Streicker Bridge represents successful validation of the method. The final part of validation and comparison with various codes is given in the next subtask description.

Subtask 3.2: Exploring design codes for numerical simulation of prestress losses for Streicker Bridge and comparison to values from Subtask 3.1

The three-year prestress force loss is determined at every cross-section equipped with sensors using procedure developed in Subtask 2.2. The results are given in Figure 13. The prestress loss decrease is shown as a change in the density of lines over time.

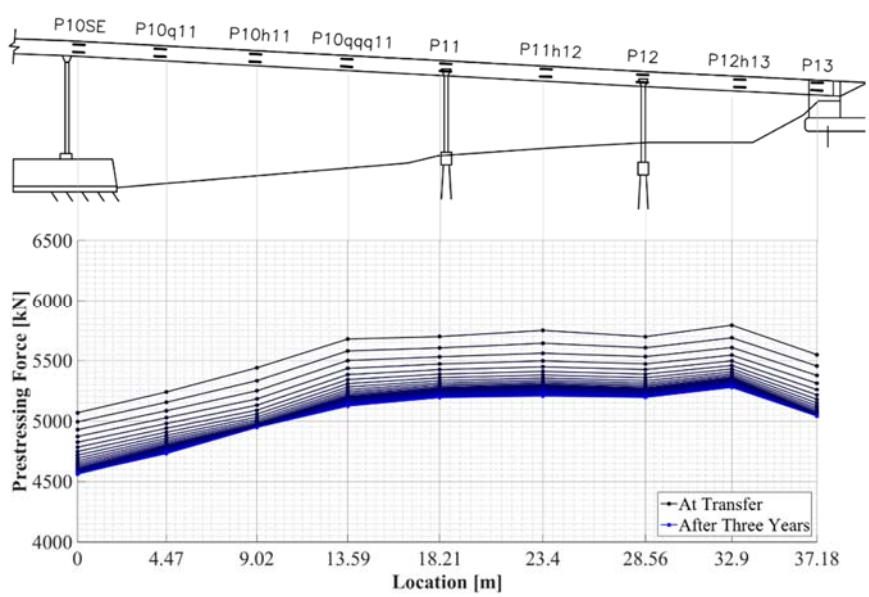

Figure 13. Monthly plots of three-year prestress loss, 2009 (black) to 2012 (blue).

Figure 14 presents the final prestress force distribution after three years, including 80% confidence interval. The latter is determined by accounting all uncertainties (sensor location, accuracy of monitoring system, etc.), as given in Equation (17). In addition, Figure 14 shows four estimates for prestress losses based on various codes: (1) the designer estimate based on CEB-FIP model for shrinkage and creep calculations [7] and on AASHTO LRFD Refined estimate for strand relaxation [8], (2) the estimate based on PCI Simplified Method [9], (3) the estimate based on AASHTO Approximate Method [8], and (4) the estimate based on AASHTO LRFD Refined Method [8]. The last three methods (2-4) were taken using recommendations given in the Guide to Estimating Prestress Loss, a report by Joint ACI-ASCE Committee 423 [10]. All four estimates yield comparable results presented in Figure 14 and Table 2.

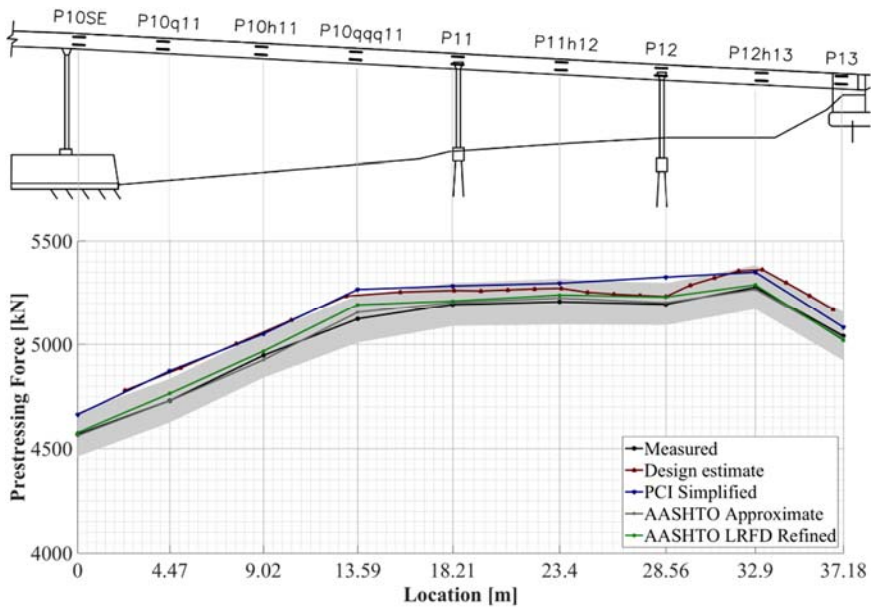

Figure 14. Comparison between prestress force distributions determined from monitoring and four design codes after three years (2009 – 2012); 80% confidence interval for monitoring data is shown in gray color.

Figure 14 and Table 2 demonstrate that prestress forces determined based on measurement is in general lower than that determined by codes. However, the code estimates are predominantly within the 80% confidence interval of prestress force determined based on measurements, except at few instances. In overall, this leads to conclusion that measured prestress losses do not significantly exceed design estimates. While all four codes result in similar estimates, it is worth noting that AASHTO Approximate Method and AASHTO LRFD Refined Method yield slightly more conservative results than the two other methods.

Table 2 presents confidence levels calculated for each of the four code estimates at each of the nine locations equipped with sensors. The confidence levels are calculated assuming Gaussian probability density function for the measured values, taking the determined prestress loss as the mean and the uncertainty as the standard deviation. The confidence levels show the probability that the measured prestress loss and the code estimates are not different. The following common thresholds on are proposed for two-tailed analysis:

⩽2% there is a highly significant difference between the values determined from measurements and those estimated using codes;

⩽10% there is a significant difference between the values determined from measurements and those estimated using codes;

⩽20% there is a marginally significant difference between the values determined from measurements and those estimated using codes;

>20% there is no significant difference between the values determined from measurements and those estimated using codes.

The confidence level threshold of 20% was proposed based on experience and used in a previous work [11]. Cells highlighted in gray color in Table 2 indicate values that are below the threshold (i.e., showing some degree of inconsistency between measured values and those determined using codes).

Table 2. Prestress loss determined from measurements and the code estimates using PCI Simplified Method, AASHTO Approximate Method, AASHTO LRFD Method, and Design*.

	P10SE	P10q11	P10h11	P10qqq11	P11	P11h12	P12	P12h13	P13
Measured Loss (kN)	499.9	509.5	493	554.3	504.6	542	502.4	514.6	508
Uncertainty (kN)	81.6	80.9	81.9	87.6	80.1	85.7	78.2	82.0	90.1
PCI Simplified Estimate (kN)	411.0	374.0	398.7	419.3	422.4	461.1	378.8	451.1	473.9
Confidence Level	28%	9%	25%	12%	31%	34%	11%	44%	71%
AASHTO Approximate Estimate (kN)	511.8	517.1	523.5	531.2	503.4	533.3	503.4	533.9	526.6
Confidence Level	88%	93%	71%	79%	99%	92%	99%	81%	84%
AASHTO LRFD Refined Estim. (kN)	498.0	482.2	481.4	493.5	495.6	518.5	475.2	512.2	536.6
Confidence Level	98%	74%	89%	49%	91%	78%	73%	98%	75%
Design Estim.* (kN)	413.5	384.0	395.0	426.1	444.9	484.5	473.0	421.3	416.9
Confidence Level	29%	12%	23%	14%	46%	50%	71%	26%	31%

* Design estimates interpolated because they are not available at the instrumented locations

This task is concluded by determining the influence of seasonal variations in temperature and humidity cause (see Figures 10 and 11) to prestress force. Table 3 shows compares the seasonal components of the prestress losses with the non-seasonal components. Table 3 shows that the effects are more pronounced in the shorter spans (P11-P12 and P12-P13), which can be preliminary explained by higher bending stiffness (i.e., generation of higher stress and strain due to restraints to thermal effects). Generally, seasonal effects do not exceed 8% of non-seasonal effects.

Table 3. Influence of seasonal effects to prestress loss.

	Prestress Loss (kN)	
Sensor Location	**Non-seasonal Component**	**Seasonal Component**
P10SE	499.9	18.7 (3.7%)
P10q11	509.5	11.4 (2.2%)
P10h11	493.0	18.3 (3.7%)
P10qqq11	554.3	26.4 (4.8%)
P11	504.6	33.9 (6.7%)
P11h12	542.0	29.1 (5.4%)
P12	502.4	33.0 (6.6%)
P12h13	514.6	30.1 (5.8%)
P13	508.0	20.0 (3.9%)

CONCLUSIONS

Several major conclusions can be drawn from this project:

1. Long-term strain and temperature monitoring in civil structures and infrastructure is becoming increasingly important given that they are supposed to last several decades and that during that time they are exposed to significant thermal and mechanical loads. Consequently, accurate long-term measurements are essential in order to derive accurate conclusions regarding long-term structural performance and health condition.

2. Long-term monitoring of prestressed force / losses in structures is becoming increasingly important as the use of prestressed concrete increases and is typically performed in conjunction with development of new cementitious materials, such as high performance concrete that relies on and amplifies the benefits of prestressed construction.

3. This research presents two novel, practical sets of methods for SHM:
    a. Methods for on-site validation of long-term strain and temperature measurements from sensors installed on structure.
    b. Method for determination of long-term prestress losses in beam-like structures.

4. The method for on-site validation of long-term temperature measurements that features:
    a. Modeling the relationship between the internal structure's temperature (measured by sensors) and the ambient temperature assumed to be accurate in the long term (measured by external neighboring weather tower) over a training period during which the sensor is assumed to measure accurately; model is based on linear regression with moving average;
    b. Measurements occurring after training period are then predicted using the model and compared to sensor measurements; deviations between the predictions and measurements are evaluated and classified as malfunction or drift; the method describes the processes of model selection and setting thresholds for these two issues.
    c. The method is independent of the type of temperature sensors used.

5. The method for on-site validation of long-term strain measurements could be created only indirectly, using correlations between sensor measurements; this indirect approach

was imposed by limitations of available SHM system; although the method showed satisfactory performance, it can be improved by adding redundant independent strain sensors (see recommendations).

6. The method for the long-term monitoring of prestress force/loss distribution along beam-like structures is based on the use of strain measurements from embedded long-gauge fiber optic sensors. The strengths of the method are:
    a. It uses strain at the centroid of stiffness of the cross-section as the main parameter to calculate the prestress force, which makes the method robust to the effects of operational load and seasonal variations;
    b. It accounts for uncertainties, which makes possible probabilistic comparison to code/design estimates;
    c. It is applicable wide range of beam-like structures beyond bridge girders.

7. The methods were successfully validated through application on Streicker Bridge on the Princeton University campus; the bridge was instrumented with SHM system in 2009, and 7-year data was used in the project:
    a. Validation confirmed the reliability in identifying both fully functional and problematic sensors; for problematic sensors it was possible to ascertain the type of malfunction, even though the weather tower was 10 miles away from the bridge.
    b. Long-term prestress force distribution along the bridge, as well as long-term losses were successfully determined; results showed that although the design and code estimates are generally close to the prestress losses obtained using sensor measurements, they are not necessarily conservative; thus, although several studies presented in literature indicated that prestress losses in HPC are lower than those in ordinary concrete, the results from Streicker Bridge showed that this should not be a general conclusion.
    c. The result from this case study confirms the importance of monitoring prestressed concrete structures rather than carrying out generalized conclusions about all structures based on literature review.
    d. Specific conclusion for the Streicker Bridge is that most long-term prestress losses occured during the first 3 years (94%–100%).

Publications resulting from the project:

<u>Journal Papers</u>

1. Abdel-Jaber, H., Glisic, B. (2019). Monitoring of prestressing forces in prestressed concrete structures - an overview, Structural Control and Health Monitoring (submitted, under review).

2. Abdel-Jaber, H., Glisic, B. (2018). Monitoring of long-term prestress losses in prestressed concrete structures using fiber optic sensors, Structural Health Monitoring (Online First doi 10.1177/1475921717751870, in press).

3. Abdel-Jaber, H, Glisic, B. (2016). Systematic method for the validation of long-term temperature measurements, Smart Materials and Structures, 25, art. no. 125025 (12pp).

4. Abdel-Jaber, H., Glisic, B., (2016). Structural Health Monitoring Methods for the Evaluation of Prestressing Forces and Prerelease Cracks Methods, Frontiers in Built Environment - Structural Sensing, 2, art. no. 20 (9pp).

Conference papers and presentations:

1. Abdel-Jaber, H., Glisic, B. (2017). Method for Validation of Long-Term Temperature measurements from Sensors, 39th IABSE Symposium, September 19-23, Vancouver, Canada.

2. Abdel-Jaber, H., Glisic, B. (2017). Prestress Loss Monitoring Using Long-Gauge Fiber Optic Sensors, 39th IABSE Symposium, September 19-23, Vancouver, Canada.

3. Reilly, J., Abdel-Jaber, H., Yarnold, M., Glisic, B. (2017). Approximating the coefficient of thermal expansion of concrete using time periods of uniform thermal gradient, Proc. SPIE 10169, Nondestructive Characterization and Monitoring of Advanced Materials, Aerospace, and Civil Infrastructure, and Transportation, art. no. 1016929.

4. Abdel-Jaber, H., Glisic, B. (2017). Monitoring of prestress losses using long-gauge fiber optic sensors, Proc. SPIE 10170, Health Monitoring of Structural and Biological Systems 2017.

5. Abdel-Jaber, H., Glisic, B. (2016). Evaluation of prestressing forces and pre-release cracks using fiber optic sensors, ACI Fall Convention 2016.

6. Glisic, B., Sigurdardottir, D.H., Abdel-Jaber, H., Kliewer, K., Li, X., Reilly, J. (2016). Recent contributions to strain-based structural health monitoring using long-gauge fiber optic sensors – an overview, CSHM-6, the 6th workshop on Civil Structural Health Monitoring, Belfast, UK, on conference CD.

7. Abdel-Jaber, H., Glisic, B. (2016). Validation of long-term measurements from FBG sensors, Proc. SPIE 9805, Health Monitoring of Structural and Biological Systems 2016, 980523.

8. Reilly, J., Abdel-Jaber, H., Yarnold, M., Glisic, B. (2016). Identification of steady-state uniform temperature distributions to facilitate a temperature driven method of Structural Health Monitoring, Proc. SPIE 9805, Health Monitoring of Structural and Biological Systems 2016, 980521.

RECOMMENDATIONS

This project created methods for validation of long-term strain and temperature measurements, and determination of prestress force/loss distribution. The following recommendations are proposed based on experience and test results from the project:

1. Literature review and this project demonstrated that strain and temperature measurements are the most effective in determining the long-term prestress force/losses

distribution along beam-like structures; to make the SHM system the most effective, it is recommended to start monitoring with the birth of the structure, i.e., to embed the snsors in concrete during construction.

2. Having two parallel strain and temperature sensors installed in each instrumented cross-section (one above and one below centroid) is minimum requirement; however, the budget permitting, it is recommended to install at least one more strain and temperature sensor across the depth of the cross-section, to better understand and account for thermal gradients, and to improve accuracy in determination of strain at the centroid.

3. The locations of cross-section to be instrumented with sensors should be those with maximum positive and negative bending moments (approximately in the middle of spans or above supporting columns of the beam structure); however, it is important to also instrument few inflection points for the control purposes.

4. To improve accuracy and robustness of long-term validation of strain and temperature measurements, it is recommended to embed redundant probe strain and temperature sensors at few locations; these sensors should be based on technology which is different from the original SHM system, yet having proven performance in long terms.

5. To improve accuracy and robustness of long-term validation of temperature measurements, it is recommended to install calibrated external sensor (e.g., weather station) as close to monitoring structure as possible.

6. For the best results in long-term validation of strain and temperature measurements, training period of 1-2 years is recommended, so the seasonal changes are included in the training set.

REFERENCES

1. FHWA. National Bridge Inspection Standards. 2004 [cited 2015 12/10]; Available from: https://www.gpo.gov/fdsys/pkg/FR-2004-12-14/pdf/04-27355.pdf

2. NBI, NBI ASCII Files. 2014 [cited 2015 12/10]; Available from: https://www.fhwa.dot.gov/bridge/nbi/ascii.cfm

3. Baran, E., Shield, C., French, C., Wyffels,T. (2004). "Analysis of the Effects of Vertical Pre-Release Cracks on Prestressed Concrete Bridge Girders" PCI Journal.

4. Akaike H 1973 Information theory and an extension of the maximum likelihood principle 2nd Int. Symp. On Information Theory pp 267–81

5. Schwarz G 1978 Estimating the dimension of a model Ann. Stat. 6 461–4.

6. Burnham K P and Anderson D R 2002 Model Selection and Multimodel Inference: A Practical Information-Theoretic Approach (New York: Springer)

7. ISO/IEC. International vocabulary of metrology—basic and general concepts and associated terms, 3rd ed. VIM, ISO/IEC Guide 99-12:2007. Geneva: International Organization for Standardization, 2007.

8. AASHTO. AASHTO LRFD bridge design specifications, 6th ed. Washington, DC: American Association of State Highway and Transportation Officials, 2012, 1661 pp..

9. Prestressed Concrete Institute (PCI). PCI design handbook, 7th ed. Chicago, IL: Precast/Prestressed Concrete Institute, 2010, 804 pp.

10. Joint ACI-ASCE Committee 423. Guide to estimating prestress loss. Farmington Hills, MI, 2016, https://www.concrete.org/Portals/0/Files/PDF/Previews/423.10R-16_preview.pdf

11. Abdel-Jaber H and Glisic B. A method for the on-site determination of prestressing forces using long-gauge fiber optic strain sensors. Smart Mater Struct 2014; 23(7): 75004.